Scheme 1: one step search: In this scheme, each reflection coefficient is quantised independently. The analysis steps are as follows. The best reflection coefficient is obtained by searching the codebook using eqn. 7, then from eqn. 5 the prediction errors are updated using the quantised reflection coefficient. These steps are repeated until all reflection coefficients have been fixed.

Scheme 2: two step search: In this scheme, two reflection coefficients are quantised in a single step. By evaluating eqn. 5 for two consecutive steps, we have

$$\begin{aligned}\alpha_0^{m+2} &= \alpha_0^m(1 + k_{m+1}^2)(1 + k_{m+2}^2) \\ &\quad - 2k_{m+1}(1 + k_{m+2}^2)\beta_1^m - 2k_{m+2}\beta_2^m \\ &\quad - 2k_{m+1}^2 k_{m+2}\beta_0^m + 4k_{m+1}k_{m+2}\alpha_1^m \end{aligned} \qquad (8)$$

The minimum of α_0^{m+2} is achieved by searching the quantisation tables for k_{m+1} and k_{m+2} in a single step. Once the best k_{m+1} and k_{m+2} are found, they are kept constant for the remaining analysis steps. This scheme requires more computation than scheme 1 as all combinations of two consecutive tables have to be searched.

Scheme 3: one step search with optimum path to previous stage: In this scheme, the selection of the codeword in each stage of analysis is deferred until the end of the computation loop. An array is used to hold the prediction error for each codeword in the previous stage. For each codeword in the present stage, the prediction error is obtained by selecting the minimum of the prediction errors generated from all possible paths to the previous stage and the path that generates the lowest prediction error is memorised. At the end of the analysis, the minimum from the stored prediction errors is chosen and a backtracking technique is applied to locate the index of each quantised coefficient in the table. This scheme, however, requires more computation and memory storage than schemes 1 and 2.

Simulation results: In this Section, the in-loop quantisation schemes are tested with real speech data generated from various speakers including male and female speakers. The speech signal is bandlimited to 3·4 kHz and is sampled at 8 kHz. A 32 ms Hamming window is used for autocorrelation analysis. The analysis frame size is 20 ms and the LPC order is 8. The quantisation tables for each stage of reflection coefficient are independently trained by using a global optimal design procedure based on dynamic programming techniques.[4] Several bit allocation schemes for the quantisation tables are used. The bit allocation is somewhat arbitrary, however it takes into account the weighting on dominant coefficients as this is a common practice for scalar quantisation of reflection coefficients. In comparing the long-term quantisation distortion, the averaged likelihood ratio distortion measure is employed,[5] which is defined as $d(\text{dB}) \simeq 6{\cdot}142\sqrt{(d_{LR})}$ where $d_{LR} = \alpha/\alpha_m - 1$, with α being the prediction error energy associated with the quantised coefficients

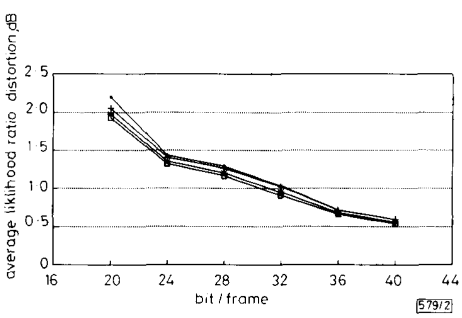

Fig. 2 *Plots of quantisation distortion for various schemes*

—●— scalar
—+— 1 step
—•— 2 step
—□— 1 step optimal

and α_m being the prediction error energy associated with unquantised coefficients. In practice, α can be calculated by going through the lattice analysis as described previously using the quantised reflection coefficients. Fig. 2 illustrates plots of the averaged likelihood ratio distortion achieved for various quantisation schemes against the coding bit rates. From these plots, we see that the one step search with optimum path (scheme 3) achieves the lowest distortion. The two-step search (scheme 2) provides the second lowest distortion. Even with a simple one-step search (scheme 1) the improvement on quantisation distortion is quite significant. We also note that the improvements are more significant when the bit rate is low.

Conclusion: An algorithm for lattice analysis with quantised reflection coefficients is introduced, and methods for in-loop quantisation of reflection coefficients are proposed. Three searching methods have been studied and the one step search with an optimum path to the previous stage provides the largest improvements in quantisation distortion.

C.-F. CHAN
K.-W. LAW

Department of Electronic Engineering
City Polytechnic of Hong Kong,
83 Tat Chee Avenue, Kowloon, Hong Kong

13th August 1991

References

1 GRAY JR., A. H., and MARKEL, J. D.: 'Digital lattice and ladder filter synthesis', *IEEE Trans.*, 1973, **AU-21, 6,** pp. 491–600
2 VISWANATHAN, V. R., and MAKHOUL, J.: 'Quantization properties of transmission parameters in linear predictive systems', *IEEE Trans.*, June 1975, **ASSP-23,** pp. 309–321
3 LE ROUX, J., and GUEGUEN, C.: 'A fixed point computation of partial correlation coefficients', *IEEE Trans.*, June 1977 **ASSP-25,** pp. 257–257
4 SOONG, F. K., and JUANG, B. H.: 'Optimal quantization of LSP parameters'. Proc. ICASSP-88, 1988, pp. 394–797
5 TRIBOLET, J. M., RABINER, L. R., and SONDHI, M. M.: 'Statistical properties of an LPC distance measure', *IEEE Trans.*, October 1979, **ASSP-27** pp. 500–558

DFB ACTIVE FILTER/DETECTOR FOR MULTICHANNEL FSK OPTICAL TRANSMISSION

Indexing terms: Active filters, Detectors, Distortion, Optical transmission, Optical filters, Optoelectronics

In a DFB laser amplifier, used simultaneously as narrowband optical filter and detector in O-FDM systems, the increase of the input optical power induces distortion of the filter transfer function. The effect of such a distortion on the receiver sensitivity and dynamic range has been investigated in a 155 Mbit/s FSK direct detection experiment. A two-channel experiment is also reported for the first time. Owing to the effect of interference between the two channels, it has been found that a minimum channel spacing of about 15 GHz is required to maintain the bit error rate below 10^{-9}.

Introduction: Narrowband tunable optical filters will be key devices for future networks based on optical frequency division multiplexing (O-FDM).[1] Recently it was found that Fabry-Perot (FP), distributed feedback (DFB) and distributed Bragg reflector (DBR) semiconductor lasers, operating just below the lasing threshold, can be effectively used as narrowband tunable optical filters.[2–4] Furthermore, because the electrical voltage across the junction of the laser amplifier is related to the optical signal through the depletion of the carrier density, the device can operate simultaneously as a high-sensitivity photodetector, thus providing a much simplified receiver structure.[2,5]

Optical signal transmission experiments using a resonant laser amplifier as an active filter/photodetector (AFPD) have been reported at bit rates of 100 Mbit/s, 250 Mbit/s[5] and, recently, at 1·5 Gbit/s.[6] However, theoretical analysis has revealed that both the static and dynamic characteristics of a resonant laser amplifier are closely related to the bias level of the optical amplifier and to the power level of the optical input signal.[4] The transfer function of an optical amplifier is particularly sensitive to the input optical power when the amplifier is biased near its lasing threshold. This effect might result in the degradation of the system performance if the operating conditions were not optimised. Moreover, because the investigation of the laser amplifier AFPD is mainly aimed at future applications of the O-FDM in the optical networks, a further experimental study on the multichannel transmission system is needed.

We report, for the first time, the results of a two channel 155 Mbit/s FSK direct detection experiment using a DFB laser amplifier as a narrowband AFPD (DFB-AFPD). By measuring the system bit error rate (BER) for different operating conditions of the laser amplifier, criteria for optimisation are outlined. System performance degradation due to the interference between channels is also evaluated. A serious BER deterioration is observed when the channel spacing is less than 15 GHz. This sets a limit to the channel density that could be reached in O-FDM networks making use of currently available DFB laser amplifier as AFPDs.

Experimental setup: The experimental setup is shown in Fig. 1. Two commercial single-electrode DFB laser dioses are used as

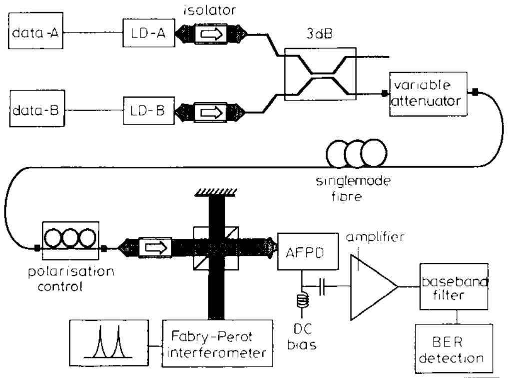

Fig. 1 *Experimental setup*

transmitters. The light from each laser is coupled into a 3 dB fibre coupler through an optical isolator providing 70 dB isolation. A polarisation maintaining directional coupler is used to obtain the same state of polarisation for the two laser fields at the input of the fibre line. Finally, a variable optical power attenuator provides precise control of the optical power transmitted to the receiver.

At the receiver side, the signal is coupled into another commercial DFB laser, operating just below threshold and acting as a narrowband optical filter. The electrical signal is tapped from the electrode of the laser amplifier through a bias tee. To monitor both the incoming and the amplified optical spectrum, a beam splitter taps part of the reflected light and sends it to a Fabry-Perot interferometer. Another optical isolator is used to prevent spurious feedback to the optical amplifier. The detected electrical signal from the AFPD is amplified by about 60 dB, using a 50 Ω amplifier. Finally, a suitable baseband filter is used before the BER counter.

Results and discussion: In the single channel experiment, the 155 Mbit/s FSK optical signal is obtained by directly modulating the injection current of laser A. Pre-equalisation of the electrical data signal is used to compensate for the nonuniform FM response of the transmitters.[7]

When the input optical power is increased, the DFB-AFPD transfer function exhibits a strong distortion.[3] The increase of the amplified optical power decreases the carrier density and increases the refractive index inside the cavity of the amplifier thus resulting in a shift of the filter resonance peak towards longer wavelengths and simultaneously in an asymmetrical broadening of the filter response.

The effect of this distortion on the system performance can be evaluated by measuring the BER against input optical power for different bias levels of the DFB-AFPD; corresponding results are shown in Fig. 2. A large frequency deviation

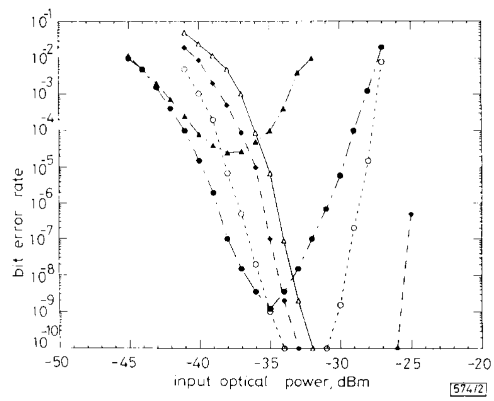

Fig. 2 *Measured BER deterioration due to distortion of transfer function in DFB laser amplifier, for 155 Mbit/s FSK transmission (NRZ 2^7-1 PRBS)*

I is injection current of laser amplifier, and I_{th} threshold current

I/I_{th}
—△— 95·2%
—◆— 96·4%
—○— 97·6%
—●— 98·8%
—▲— 100%

(typically 6 GHz) between marks and spaces is adopted, and the DFB-AFPD acts as a single filter detector. The received optical power is measured before the coupling lens of the AFPD, giving a conservative estimate of the system sensitivity. It is worth noting that BER degradation is observed both with small and large input optical signals. A low BER is measured in a limited range of the input optical signal level; this dynamic range of the DFB-AFPD receiver can be enlarged by reducing the bias current of the optical amplifier; however this is achieved with a sacrifice in system sensitivity. The tradeoff between the input signal dynamic range and the system sensitivity is the key for the optimisation of the receiver performance in this kind of systems.

To demonstrate the feasibility of this filtering technique in an O-FDM network, a two channel transmission experiment has been subsequently carried out. The effect of interference arising from the adjacent channel has been evaluated by performing sensitivity measurements varying the position of channel B with respect to channel A from −20 to 20 GHz. The two transmitter lasers are FSK modulated by 155 Mbit/s data streams with about 6 GHz frequency deviation, and both emit the same optical power.

Fig. 3 shows the BER for one channel against the relative frequency displacement of the other channel. To obtain the results of Fig. 3 we have used three different bias levels for the optical amplifier. For each bias level, an optimised input power value was used according to Fig. 2 to minimise the BER. The three different operating conditions exhibit essentially the same BER behaviour, as shown in Fig. 3. To maintain the BER below 10^{-9}, the adjacent channel needs to be kept 10 GHz away at the long wavelength side and 15 GHz away at the short wavelength side. The asymmetry is due to the asymmetric transfer function of the optical amplifier in the non-negligible input optical power regime. Because a very sharp BER deterioration occurs when the channel spacing is less than 15 GHz, this sets the lower limit to the channel density for O-FDM network applications of the DFB-AFPD.

Conclusion: The effect of the optical power level entering a DFB amplifier-filter-detector on the receiver performance has been experimentally characterised in a 155 Mbit/s FSK direct detection transmission system; this effect affects the sensitivity and results in a limited dynamic range, whose width depends on the bias level. Such a limitation can be relaxed to some

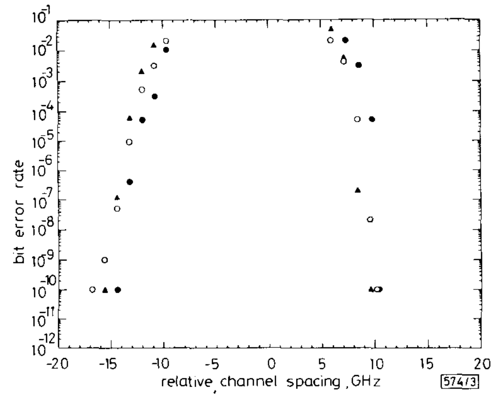

Fig. 3 *Measured BER against channel spacing in two-channel 155 Mbit/s FSK (NRZ 2^7-1 PRBS) transmission experiment*

I is injection current of laser amplifier, I_{th} threshold current, P_i input optical power

▲ $I = 0{\cdot}952 I_{th}$, $P_i = -26$ dBm

● $I = 0{\cdot}964 I_{th}$, $P_i = -30$ dBm

○ $I = 0{\cdot}976 I_{th}$, $P_i = -33$ dBm

extent by reducing the bias level of the laser amplifier, but at the expense of the system sensitivity. In the following two-channel transmission experiment the effect of channel spacing on the system performance was also characterised, resulting in a spacing lower bound of about 15 GHz to maintain the system BER below 10^{-9}. This channel density approaches that attainable in heterodyne receivers with the same modulation format, but is obtained with a much simple receiver structure.

Acknowledgments: This work has been partially supported by SIB and ITALTEL. The authors would like to thank F. Delpiano for the device packaging, and A. Graziani and V. Seano for the design and construction of the equalisation circuits and baseband filter.

R. HUI
N. CAPONIO
P. GAMBINI
M. PULEO
E. VEZZONI

13th August 1991

CSELT-Centro Studi e Laboratori Telecomunicazioni S.p.A.
Via G. Reiss Romoli 274, I-10148 Torino, Italy

References

1 KAMINOW, I. P.: 'FSK with direct detection in optical multiple-access FDM networks', *IEEE J. Sel. Areas Commun.*, 1990, **SAC-8,** pp. 1005–1014

2 NAKAJIMA, H.: 'High-speed and high-gain optical amplifying photodetection in a semiconductor laser amplifier', *Appl. Phys. Lett.*, 1989, **54,** pp. 984–986

3 MAGARI, G., KAWAGUCHI, H., OE, K., and FUKUDA, M.: 'Optical narrow-band filters using optical amplification with distributed feedback', *IEEE J. Quantum Electron.*, 1988, **QE-24,** pp. 2178–2190

4 CHOA, F. S., and KOCH, T. L.: 'Static and dynamical characteristics of narrow-band tunable resonant amplifiers as active filters and receivers', *J. Lightwave Technology*, 1991, **LT-9,** pp. 73–83

5 KOCH, T. L., CHOA, F. S., HEISMANN, F., and KOREN, U.: 'Tunable multiple quantum-well distributed Bragg reflector lasers as tunable narrow-band receivers', *Electron. Lett.*, 1989, **24,** pp. 890–892

6 CHAWKI, M. J., AUFFRET, R., and BERTHOU, L.: '1·5 Gbit/s FSK transmission system using two electrode DFB laser as a tunable FSK siscriminator/photodetector', *Electron. Lett.*, 1990, **26,** pp. 1146–1147

7 GAMBINI, P., PULEO, M., CAPONIO, N., and VEZZONI, E.: 'Impact of DFB-LD FM response distortion, in amplitude and phase, on FSK coherent systems', *in* 'Conference Record' (ICC'91, Denver, USA, June 1991) pp. 334–337

DIFFERENTIAL SCANNING CALORIMETRY STUDIES ON EUTECTIC (Sn63/Pb37) SOLDER PASTE AND POWDER FOR SURFACE MOUNT TECHNOLOGY

Indexing terms: Surface mount technology, Measurement, Differential scanning calorimetry, Solders

The properties of eutectic solder paste (Sn63/Pb37) in an RMA flux and solder powder have been investigated using differential scanning calorimetry. The results show that the melting point for both the paste and powder samples occurs at 182°C and also the effects of supercooling occurs for both the paste and the powder samples. The supercooling results are of vital importance in the modelling of the thermal processes for electronics manufacture using surface mount technology.

Introduction: The conventional plated-through-hole (PTH) methods of assembling electronic components have virtually reached their limits as far as improvements in cost, weight, volume and reliability of manufacturing of electronics circuits are concerned. The recent change of manufacturing strategy to mounting components on boards rather than through them has resulted in changes in component packaging shapes and sizes, changes to fully automated component handling, new component attachment methods using screen printed solder pastes or conductive adhesives, innovative changes in board design algorithms and changes in the requirements of post-assembly cleaning, testing and inspection. It is widely realised[1] that work is required to establish the choice of preferred termination and pad designs, joint geometry, soldering parameters and joining process parameters for high volume manufacture and high reliability joint production. The current trends towards fine pitch and high joint counts per board have resulted in a larger proportion of SMDs requiring rework. The defect rate must therefore be reduced to maintain and improve first-off production yields. Solder paste as a joining material provides electrical, thermal and mechanical functions in an electronics assembly. The performance and quality of solder paste are crucial to the integrity of a solder joint, which in turn is vital to the overall function of the assembly. The aims of this work are to measure and investigate the properties of the eutectic solder paste and powder used in the surface mount industries (the samples have been supplied by Alpha Metals Inc.). In this work, the samples have been prepared for differential scanning calorimetry (DSC) experiments to measure the thermal properties and also to investigate any phenomena which may arise from the thermal cycling during the experiments. It is also one of the aims of this study to obtain accurate data from these measurements of thermal properties that would enable the formulation of a thermal model for IR reflow soldering for surface mount assemblies.

Experimental detail: Solder paste supplied by α-Metals (Fine Line Paste: 63/67 RMA390DH3 89-3-90 250 GRM, received 30/1/91) was predried by using a hot air blower. Also, solder powder (63/37 PWD 3 300 Control Paste Powder Lot No.: B1082) was supplied by the same company (REF. No.: 01 SP 0925). The drying of the paste was carried out to ease sample preparation, weighting and loading into the aluminium sample pans. A typical pan plus lid weighs between 22·69 to 23·20 mg. The sample was isolated from the surroundings by covering the top with an aluminium lid and by pushing the edges of the sample pan inwards and downwards. A total weight could then be obtained. The first DSC experiment was optimised between 30°C to 250°C with empty sample holders to obtain a baseline.

Results: The following observations can be made after viewing and comparing the Figs. 1–3. First, the melting point of both the paste and powder samples is at 182 ± 1°C. Secondly, the endothermic peak shows a slight broadening after reheating of the paste sample Paste 1 and this can be observed in Fig. 1. Also, the melting and solidification point occurs at different temperature for both paste and powder, hence showing the